articles

molecular pharmaceutics

Structure and Concentration Changes Affect Characterization of UGT Isoform-Specific Metabolism of Isoflavones

Lan Tang,[†,‡,§] Rashim Singh,[‡,§] Zhongqiu Liu,[†] and Ming Hu*[,†,‡]

Department of Pharmaceutics, School of Pharmaceutical Sciences, Southern Medical University, Guangzhou, Guangdong, China, and Department of Pharmacological and Pharmaceutical Sciences, College of Pharmacy, University of Houston, 1441 Moursund Street, Houston, Texas 77030

Received December 5, 2008; Revised Manuscript Received May 21, 2009; Accepted June 22, 2009

Abstract: We characterized the isoform specific glucuronidation of six isoflavones, genistein, daidzein, glycitein, formononetin, biochanin A and prunetin, using 12 expressed human UGTs and human intestinal and liver microsomes. The results indicated that these isoflavones are metabolized most rapidly at three different concentrations by one of these four UGT isoforms: UGT1A1, UGT1A8, UGT1A9 and UGT1A10. Furthermore, glycitein was usually metabolized the fastest whereas prunetin the slowest. Using the rates of metabolism by 12 UGT isoforms as a means to establish the metabolic "fingerprint", we found that each isoflavone had distinctive concentration-dependent patterns. Determination of kinetic parameters of glucuronidation using genistein and prunetin indicated that the distinct concentration-dependent metabolic patterns were the result of differences in K_m and V_{max} values. We then measured how well metabolic "fingerprinting" predicted metabolism of these isoflavones by human intestinal and liver microsomes. We found that the prediction was rather successful for five isoflavones in the liver microsomes, but not successful in the intestinal microsomes. We propose that a newly discovered UGT3A1 isoform capable of metabolizing phenols and estrogens might be responsible for the metabolism of isoflavones such as formononetin in humans. In conclusion, the first systematic study of metabolic "fingerprinting" of six common isoflavones showed that each isoflavone has UGT isoform-specific metabolic patterns that are concentration-dependent and predictive of metabolism of the isoflavones in liver microsomes.

Keywords: UGT; glucuronidation; fingerprinting; profile; genistein; isoflavones

Introduction

Isoflavones, such as genistein, daidzein, glycitein, biochanin A, prunetin, and formononetin (Figure 1), belong to a class of phytochemicals called phytoestrogens. Natural sources of isoflavones include soy and soy foods, alfalfa sprouts, and red clover.[1,2] Soybeans have abundant amounts of genistein, daidzein, glycitein, and their glycosides.[3] On the other hand, red clover has large amounts of formononetin and biochanin A in addition to genistein, and daidzein.[4] Prunetin is mainly found in Kudzu roots, a Chinese herb found to be active against alcohol abuse.[5] Isoflavones have

* Address correspondence to Ming Hu, Ph.D., 1441 Moursund Street, Department of Pharmaceutical Sciences, College of Pharmacy, University of Houston, Houston, TX 77030. Tel: (713)-795-8320. Fax: (713)-795-8305. E-mail: mhu@uh.edu.

[†] Southern Medical University.

[‡] University of Houston.

[§] L.T. and R.S. made equally significant contributions to the project.

(1) Birt, D. F.; Hendrich, S.; Wang, W. Dietary agents in cancer prevention: flavonoids and isoflavonoids. *Pharmacol. Ther.* **2001**, *90*, 157–77.

(2) Wang, S. W.; Chen, J.; Jia, X.; Tam, V. H.; Hu, M. Disposition of flavonoids via enteric recycling: structural effects and lack of correlations between in vitro and in situ metabolic properties. *Drug Metab. Dispos.* **2006**, *34*, 1837–48.

10.1021/mp8002557 CCC: $40.75
Published on Web 06/22/2009

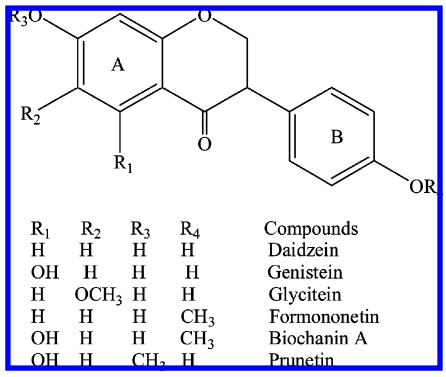

R_1	R_2	R_3	R_4	Compounds
H	H	H	H	Daidzein
OH	H	H	H	Genistein
H	OCH_3	H	H	Glycitein
H	H	H	CH_3	Formononetin
OH	H	H	CH_3	Biochanin A
OH	H	CH_3	H	Prunetin

Figure 1. Structure of model compounds. Shown in the scheme are structures of aglycon forms of six isoflavones. Isoflavones differ from flavones in that the "B" ring is at position 3 instead of position 2 of the benzopyranone or "A" ring. Conjugated phase II metabolites are usually formed on the 7-hydroxy group on the A ring and the 4′-OH group on the B ring.

been shown to possess significant biological activities ranging from anticancer to cardiovascular protective effects.[3,6,7] Their in vitro and in vivo mechanisms of action range from antioxidants to antiproliferation.[6]

Despite these claimed health benefits and demonstrated preclinical activities, there are significant challenges associated with development of isoflavones into chemopreventive and chemotherapeutic agents. The major challenge currently is their low bioavailabilities (<5%), as the result of extensive first-pass metabolism by phase II enzymes including UGTs and SULTs.[8,9] A large body of work has been done in multiple research laboratories including our own to understand the metabolic pathways of isoflavones and how they relate to poor bioavailabilities.

Our previous studies have shown that glucuronidation of isoflavones in intestine and subsequent excretion of respective glucuronides from intestine was affected by the structure of isoflavones and possibly the structure of isoflavone glucuronides, respectively.[2,10] Additional studies of isoflavones in Caco-2 cells showed that glucuronidation of isoflavones and excretion of their glucuronides were strongly influenced by their structure.[11] Our recent study indicated that prunetin might be metabolized into multiple glucuronides and that formation of a particular metabolite (e.g., prunetin-4′-*O*-glucuronide) was sometimes determined only by the presence of a specific UGT isoform (i.e., UGT1A10).[12] Therefore, systematic metabolic profiling studies utilizing expressed human UGT isoforms is of great importance in determining major isoform(s) responsible for isoflavone metabolism, determining major metabolite(s) formed by particular isoform, and predicting the major organ (site) of metabolism. The information so derived may also be used to gauge the safety and efficacy concerns which may arise from potential drug−drug interactions and genetic polymorphism. Metabolic profiling (or reaction phenotyping) may also be used to determine the likelihood of success of approaches developed to improve human isoflavone bioavailability.

The present study represents a detailed and systematic study of UGT isoform-specific metabolism of six isoflavones commonly used in studies of isoflavones in the literature: genistein, daidzein, glycitein, biochanin A, formononetin, and prunetin. As a first study of this kind, the overall goal of this research was to demonstrate the potential utilities of UGT metabolic characterization in predicting safety and efficacy of a chemical (in this case an isoflavone). Toward this goal, the first two objectives of this study were to determine if these structurally diverse isoflavones were mainly metabolized by the same set of UGT isoform(s) and to determine how changes in isoflavone structures and differences in substrate concentrations affect the UGT isoform-specific metabolism of isoflavones. Another objective was to determine if isoform specific metabolic pattern, determined from metabolic profiling, might be used to predict glucuronidation rates of isoflavones in microsomes derived from human intestine and liver, two major organs responsible for first-pass metabolism as well as recycling via enteric and enterohepatic schemes.[13,14]

(3) Kurzer, M. S.; Xu, X. Dietary phytoestrogens. *Annu. Rev. Nutr.* **1997**, *17*, 353–81.
(4) Lin, L. Z.; He, X. G.; Lindenmaier, M.; Yang, J.; Cleary, M.; Qiu, S. X.; Cordell, G. A. LC-ESI-MS study of the flavonoid glycoside malonates of red clover (Trifolium pratense). *J. Agric. Food Chem.* **2000**, *48*, 354–65.
(5) Lukas, S. E.; Penetar, D.; Berko, J.; Vicens, L.; Palmer, C.; Mallya, G.; Macklin, E. A.; Lee, D. Y. An extract of the Chinese herbal root kudzu reduces alcohol drinking by heavy drinkers in a naturalistic setting. *Alcohol.: Clin. Exp. Res.* **2005**, *29*, 756–62.
(6) Thomasset, S. C.; Berry, D. P.; Garcea, G.; Marczylo, T.; Steward, W. P.; Gescher, A. J. Dietary polyphenolic phytochemicals—promising cancer chemopreventive agents in humans? A review of their clinical properties. *Int. J. Cancer* **2007**, *120*, 451–8.
(7) Barnes, S. Soy isoflavones—phytoestrogens and what else? *J. Nutr.* **2004**, *134*, 1225S–1228S.
(8) Zubik, L.; Meydani, M. Bioavailability of soybean isoflavones from aglycone and glucoside forms in American women. *Am. J. Clin. Nutr.* **2003**, *77*, 1459–65.
(9) Hu, M. Commentary: bioavailability of flavonoids and polyphenols: call to arms. *Mol. Pharmaceutics* **2007**, *4*, 803–6.
(10) Chen, J.; Wang, S.; Jia, X.; Bajimaya, S.; Tam, V.; Hu, M. Disposition of Flavonoids via Recycling: Comparison of Intestinal versus Hepatic Disposition. *Drug Metab. Dispos.* **2005**, *33*, 1777–84.
(11) Chen, J.; Lin, H.; Hu, M. Absorption and metabolism of genistein and its five isoflavone analogs in the human intestinal Caco-2 model. *Cancer Chemother. Pharmacol.* **2005**, *55*, 159–69.
(12) Joseph, T. B.; Wang, S. W.; Liu, X.; Kulkarni, K. H.; Wang, J.; Xu, H.; Hu, M. Disposition of flavonoids via enteric recycling: enzyme stability affects characterization of prunetin glucuronidation across species, organs, and UGT isoforms. *Mol. Pharmaceutics* **2007**, *4*, 883–94.
(13) Liu, Z.; Hu, M. Natural polyphenol disposition via coupled metabolic pathways. *Expert Opin. Drug Metab. Toxicol.* **2007**, *3*, 389–406.
(14) Jeong, E. J.; Liu, X.; Jia, X.; Chen, J.; Hu, M. Coupling of conjugating enzymes and efflux transporters: impact on bioavailability and drug interactions. *Curr. Drug Metab.* **2005**, *6*, 455–68.

Materials and Methods

Materials. Daidzein and glycitein were purchased from LC Laboratories (Woburn, MA). Biochanin A, formononetin, prunetin, and genistein were purchased from Indofine Chemicals (Somerville, NJ). Expressed human UGT isoforms (Supersomes), pooled female human liver and intestinal microsomes were purchased from BD Biosciences (Woburn, MA). Uridine diphosphoglucuronic acid (UDPGA), alamethicin, β-glucuronidase, D-saccharic-1,4-lactone monohydrate, magnesium chloride, and Hanks' balanced salt solution (powder form) were purchased from Sigma-Aldrich (St Louis, MO). All other materials (typically analytical grade or better) were used as received.

Enzymatic Activities of Expressed UGTs. The incubation procedures for measuring UGTs' activities were essentially the same as published before.[12,15] Briefly, incubation procedures using microsomes or supersomes were as follows: (1) microsomes/supersomes (final concentration approximately in the range of 0.0053−0.053 mg of protein per mL as optimum for the reaction), magnesium chloride (0.88 mM), saccharolactone (4.4 mM), alamethicin (0.022 mg/mL), different concentrations of substrates in a 50 mM potassium phosphate buffer (pH 7.4), and UDPGA (3.5 mM, added last) were mixed;[16] the mixture (final volume, 200 μL) was incubated at 37 °C for a predetermined period of time (e.g., 60 min); and (3) the reaction was stopped by the addition of 50 μL of 94% acetonitrile/6% glacial acetic acid containing 100 μM testosterone as the internal standard. For UGT profiling, three concentrations, 2.5, 10, and 35 μM (40 μM for prunetin) were used. For kinetic profiling of genistein and prunetin with UGT1A1, 1A8, 1A9 and 1A10, seven substrate concentrations in the range of 1−50 μM were used.

UPLC Analysis of Isoflavones and Their Glucuronides. We analyzed six isoflavones and their respective glucuronides by using the following common method: system, Waters Acquity UPLC with photodiode array detector and Empower software; column, BEH C18, 1.7 μm, 2.1 × 50 mm; mobile phase B, 100% acetonitrile, mobile phase A, 100% aqueous buffer (2.5 mM NH_4Ac, pH 3.0); flow rate 0.5 mL/min; gradient, 0 to 0.3 min, 10% B, 0.3 to 2.9 min, 0−50% B, 2.90 to 3.2 min, 50−90% B, 3.2 to 4.0 min, 90% B; wavelength, 254 nm for isoflavones and their respective glucuronides and testosterone; and injection volume, 10 μL. Linearity was established in the range of 0.78−100 μM (total 8 concentrations) for all compounds. The LLOQ for all compounds was 0.78 μM. Analytical methods for each compound were validated for interday and intraday variation using 6 samples at three concentrations (50, 12.5, and 1.56 μM). Precision and accuracy for all compounds were in the acceptable range of 85% to 115%.

For quantification of metabolites such as genistein glucuronides, a previously published method was used.[17] This method is essentially a method that compared the peak area change in aglycon after glucuronide is hydrolyzed by β-glucuronidases that result in peak area change in glucuronides. In this method, the change in concentrations as the result of hydrolysis can be expressed as

$$\Delta C = \frac{\Delta P_{\mathrm{I}}}{a_{\mathrm{I}}} = \frac{\Delta P_{\mathrm{IG}}}{a_{\mathrm{IG}}} \quad (1)$$

where ΔP_{IG} is the change in peak areas of isoflavone glucuronide (or IG), ΔP_{I} is the change in the peak area of its corresponding isoflavone aglycon (or I) obtained from the extracted samples before and after hydrolysis, and a_{I} and a_{IG} are the slopes of the corresponding calibration curve that goes through the origin.

The term a_{IG} was expressed in terms of a_{I}, since commercial standards of isoflavone glucuronides were not available. The latter is accomplished by

$$a_{\mathrm{IG}} = \frac{\Delta P_{\mathrm{IG}}}{\Delta P_{\mathrm{I}}} \times a_{\mathrm{I}} = K \times a_{\mathrm{I}} \quad (2)$$

where K is the conversion factor of molar extinction coefficients of glucuronides to their corresponding aglycons. We performed the same experiments at three different concentrations to calculate an average K value. This conversion factor K was used to calculate the concentration of glucuronides use the standard curve of aglycons. The following is a list of the conversion factors used: biochanin A, 1.26; daidzein, 1.02; formononetin, 1.2; genistein, 1.06; glycitein, 1.25; and prunetin, 0.98. Plugging various K values into the following equation using peak areas of metabolite, the metabolite concentration (C_{IG}) can be calculated by

$$C_{\mathrm{IG}} = \frac{P_{\mathrm{IG}}}{a_{\mathrm{IG}}} = \frac{P_{\mathrm{IG}}}{K \times a_{\mathrm{I}}} \quad (3)$$

where P_{IG} is the metabolite peak area in the chromatogram.

Confirmation of Isoflavone Glucuronide Structure by LC−MS/MS. Six isoflavones and their respective glucuronides were separated by the same UPLC system but using slightly different chromatographic conditions because of mass spectrometer requirements. Here, mobile phase A was ammonium acetate buffer (pH 7.5) and mobile phase B was 100% acetonitrile with the gradient as follows: 0 to 2.0 min, 10−35% B, 2.0 to 3.0 min, 35−70% B, 3.2 to 3.5 min, 70−10% B, 3.5 to 3.7 min, 10% B. The flow rate was 0.5 mL/min. The effluent was introduced into an API 3200 Qtrap triple-quadrupole mass spectrometer (Applied Biosystem/MDS SCIEX, Foster City, CA) equipped with a TurboIon-

(15) Liu, X.; Tam, V. H.; Hu, M. Disposition of flavonoids via enteric recycling: determination of the UDP-glucuronosyltransferase isoforms responsible for the metabolism of flavonoids in intact Caco-2 TC7 cells using siRNA. *Mol. Pharmaceutics* **2007**, *4*, 873–82.

(16) CaPCure2: http://www.capcure.org/aboutprostate/statistics.html is the address for CaP Cure statistics and other relevant prostate cancer information; *CaP Cure*, 1998.

(17) Liu, Y.; Hu, M. Absorption and metabolism of flavonoids in the caco-2 cell culture model and a perused rat intestinal model. *Drug Metab. Dispos.* **2002**, *30*, 370–7.

Spray source. The mass spectrometer was operated in negative ion mode to perform the analysis of six isoflavones and their glucuronides. The main working parameters for the mass spectrometers were set as follows: ion-spray voltage, −4.5 kV; ion source temperature, 400 °C; nebulizer gas (gas 1), nitrogen, 40 psi; turbo gas (gas 2), nitrogen, 40 psi; curtain gas, nitrogen, 20 psi and minor adjustments were then made for each isoflavones. Isoflavone monoglucuronides were identified by MS and MS2 full scan modes (Figure 2).

Kinetic Analysis. Rates of metabolism in expressed human UGT isoforms and human liver and intestine microsomes were expressed as amounts of metabolites formed per min per mg protein or nmol/min/mg. Kinetic parameters were then obtained based on the profile of Eadie−Hofstee plots.[2] If the Eadie−Hofstee plot was linear, formation rates (V) of isoflavone glucuronides at various respective substrate concentrations (C) were fit to the standard Michaelis−Menten equation:

$$V = \frac{V_{max}C}{K_m + C} \quad (4)$$

where K_m is the Michaelis−Menten constant and V_{max} is the maximum rate of formation of glucuronides.

When Eadie−Hofstee plots showed characteristic profiles of atypical kinetics (autoactivation and biphasic kinetics),[18,19] the data from these atypical profiles were fit to eq 5 or 6[16] using the ADAPT II program.[20] To determine the best-fit model, the model candidates were discriminated using the minimum Akaike's information criterion (AIC)[21] value, and the rule of parsimony was applied. Therefore, using this minimum AIC estimation (MAICE), a negative AIC value (i.e., −54.2) would be considered a better representation of the data versus a set of data having a positive AIC value (i.e., 0.83).[21]

When the kinetics of enzyme reactions showed autoactivation, formation rates (V) of isoflavone glucuronides at various substrate concentrations (C) were fit to the following equation:

$$\text{reaction rate} = \frac{[V_{max\text{-}0} + V_{max\text{-}d}(1 - e^{-CR})]C}{K_m + C} \quad (5)$$

where $V_{max\text{-}0}$ is intrinsic enzyme activity, $V_{max\text{-}d}$ is maximum induction of enzyme activity, R is rate of enzyme activity induction, C is concentration of substrate, and K_m is concentration of substrate to achieve 50% of ($V_{max\text{-}0} + V_{max\text{-}d}$).

When the enzymatic reactions showed substrate inhibition kinetics (in which the substrate compound inhibits the glucuronidation velocity especially at higher concentrations), formation rates (V) of isoflavone glucuronides at various substrate concentrations (C) were fit to the following equation:

$$\text{reaction rate} = \frac{V_{max1}}{1 + (K_{m1}/C) + (C/K_{si})} \quad (6)$$

where V_{max1} is maximum enzyme activity of UGT isoform, C is concentration of substrate, K_{m1} is concentration of substrate to achieve 50% of (V_{max}) for one UGT isoform, and K_{si} is substrate inhibition constant.

Statistical Analysis. One-way ANOVA with or without Tukey−Kramer multiple comparison (posthoc) tests were used to evaluate statistical differences. Differences were considered significant when p values were less than 0.05.

Results

Confirmation of Isoflavone Glucuronide Structure by LC−MS/MS. We conducted simple LC−MS/MS studies of the metabolites to show that all glucuronides formed using the expressed human UGTs were monoglucuronides (Figure 2). We did not find any diglucuronide of isoflavones in this study. However, we occasionally identified a second minor monoglucuronide when high concentration of genistein and glycitein were used, but the peak area of the minor metabolite was usually less than 5% of the respective major monoglucuronide peak. We did not quantify the second minor monoglucuronide in this paper.

Major Isoforms Responsible for the Metabolism of Isoflavones. To determine the main UGT isoform(s) responsible for metabolizing the selected isoflavones, we incubated the isoflavones with various UGT isoforms for up to 1 h, based on the thermostability studies of specific UGT isoforms previously done in our lab.[12] We then examined the isoform specific metabolic patterns of all isoflavones, and found that there was no single UGT isoform that could metabolize all six isoflavones at the tested concentration at the most rapid rate (Figures 3−5). In fact, the top isoform kept changing according to the compounds and concentrations, and the only commonality we could identify was that the top four isoforms were always the same: UGT1A1, 1A8, 1A9 and 1A10. Additionally, 1A7 was found to be an important isoform for glycitein and prunetin. In contrast, 1A4 and 2B4 did not make a detectable contribution to the formation of any glucuronides, whereas 1A3, 1A6, 1A7, 2B7, 2B15 and 2B17 showed small but variable extent of glucuronidation of the selected isoflavones (Figures 3−5). Moreover, "fingerprints" of M1 and M2 for prunetin were significantly different especially since UGT1A9 was not able to make M2 (Figure 5). Taken together, at low concentration of 2.5 μM, the two most important isoforms were UGT1A1 and 1A9, whereas at high concentration of 35 mM, the two most important isoforms were UGT1A8 and UGT1A10 for all isoflavones except formononetin and daidzein (Figure 2).

(18) Houston, J. B.; Kenworthy, K. E. In vitro-in vivo scaling of CYP kinetic data not consistent with the classical Michaelis-Menten model. *Drug Metab. Dispos.* **2000**, *28*, 246–54.

(19) Hutzler, J. M.; Tracy, T. S. Atypical kinetic profiles in drug metabolism reactions. *Drug Metab. Dispos.* **2002**, *30*, 355–62.

(20) D'Argenio, D. Z.; Schumitzky, A. *Biomedical simulations resource*; University of Southern California: Los Angeles, 1997.

(21) Yamaoka, K.; Nakagawa, T.; Uno, T. Application of Akaike's information criterion (AIC) in the evaluation of linear pharmacokinetic equations. *J. Pharmacokinet. Biopharm.* **1978**, *6*, 165–75.

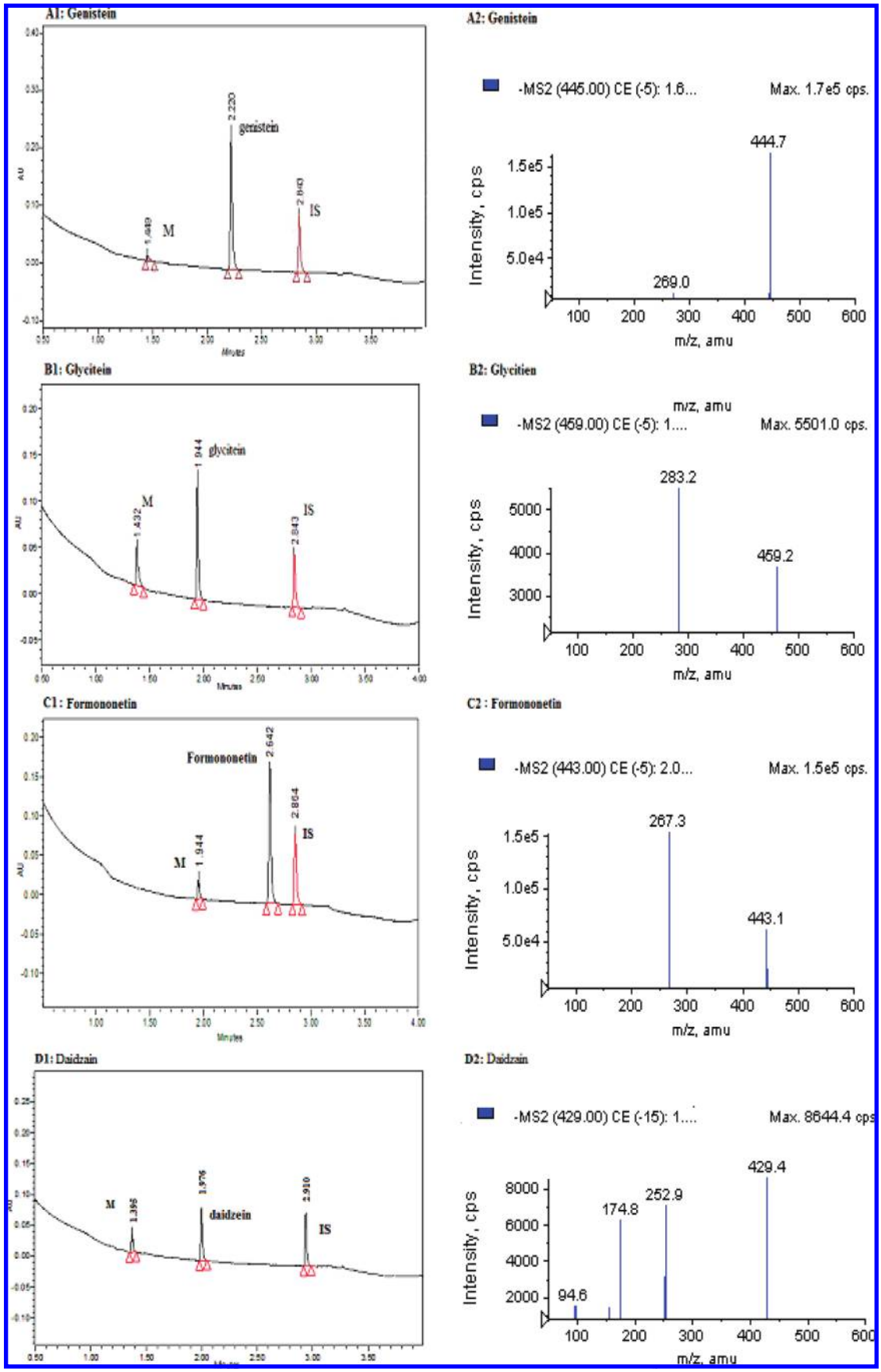
A1: Genistein
genistein
M
IS
2.220
1.489
2.843
A2: Genistein
-MS2 (445.00) CE (-5): 1.6...
Max. 1.7e5 cps.
444.7
269.0
Intensity, cps
m/z, amu
B1: Glycitein
glycitein
M
IS
1.944
1.432
2.843
B2: Glycitien
m/z, amu
-MS2 (459.00) CE (-5): 1....
Max. 5501.0 cps.
283.2
459.2
Intensity, cps
m/z, amu
C1 : Formononetin
Formononetin
M
IS
2.642
1.944
2.864
C2 : Formononetin
-MS2 (443.00) CE (-5): 2.0...
Max. 1.5e5 cps.
267.3
443.1
Intensity, cps
m/z, amu
D1: Daidzain
M
daidzein
IS
1.395
1.976
2.910
D2: Daidzain
-MS2 (429.00) CE (-15): 1....
Max. 8644.4 cps
429.4
252.9
174.8
94.6
Intensity, cps
m/z, amu

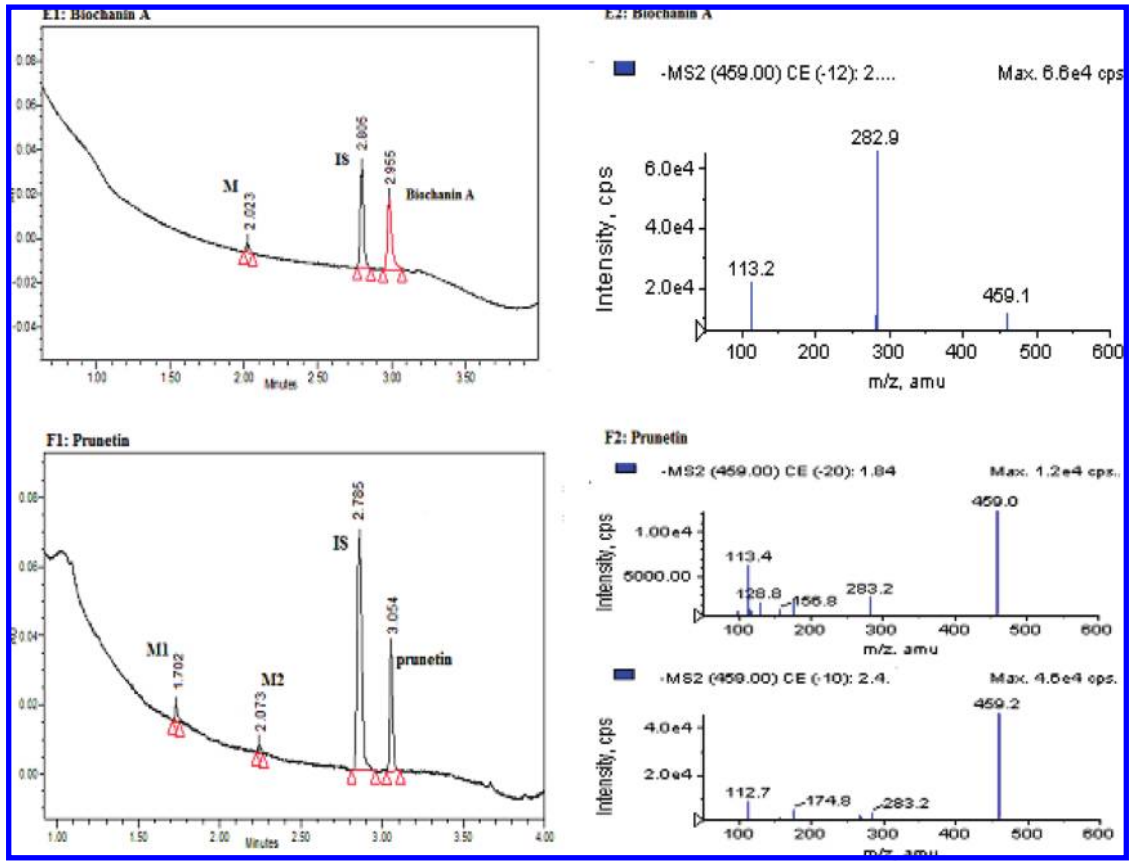

Figure 2. UPLC and LC−MS/MS profile of six isoflavones and their monoglucuronides. UPLC was used to quantify the six isoflavones and their respective monoglucuronides in the experimental samples generated after incubation with microsomes and recombinant UGT isoforms. Panels A1−F1 show the chromatograms with the retention time of each isoflavone, its respective metabolite(s) (M/M1/M2) and internal standard (IS). LC−MS/MS was used to confirm the identity of the metabolites as monoglucuronides of their parent compounds (isoflavones). Panels A2−F2 show the MS2 scan for monoglucuronide(s) of each isoflavone. Compound-specific conditions for MS (*m*/*z* and CE) are shown on each individual scan.

Isoform-Specific Metabolic Patterns of Six Isoflavones. We used 12 commercially available recombinant UGT isoforms to determine how each isoflavone was metabolized by different UGT isoforms. Since no two isoflavones shared the same metabolic pattern (shown in Figures 3−5), we assigned the pattern of metabolism of an isoflavone by the 12 UGTs as a metabolic "fingerprint" for that isoflavone. We believed that it was valuable to assign a metabolic pattern to each compound because it might be useful to predict how a compound might metabolize in a particular organ and what the possible underlying causes of drug−drug interactions might be, if any (more discussion later).

Effects of Substrate Concentration on the Isoform-Specific Metabolic Patterns. Concentration changes had significant impact on the isoform specific metabolic patterns of genistein, glycitein, biochanin A and prunetin (formation rates of prunetin-5-*O*-glucuronide or M1), because there was a significant change in the rank order of the most important isoforms as a function of concentration (Figures 3−5). For example, UGT1A9 (the largest contributor) and 1A1 were the top two isoforms responsible for genistein metabolism at 2.5 μM, but UGT1A8 became the largest contributor at 10 μM concentration, followed by UGT1A9 and UGT1A1. Concentration changes had smaller but still significant impact on the isoform specific metabolic patterns of formononetin and daidzein because there were less significant changes in the rank order as concentration changed. In the case of formononetin, UGT1A1 was always the most important but other isoforms (UGT1A8, 1A9 and 1A10) also became relevant at higher concentrations.

Concentration-Dependent Glucuronidation of Isoflavones by Four Major UGT Isoforms. Analysis of the results of glucuronidation of isoflavones by UGT1A1, 1A8, 1A9 and 1A10 showed that there were three different kinds of concentration-dependent glucuronidation profiles (Figure 6). The first profile showed that the substrate concentration had an inverse relation with the glucuronidation rate, such that the highest glucuronidation rate was achieved at the lowest substrate concentration while the lowest glucuronidation rate was achieved at the highest substrate concentration. For example, for UGT1A1, the rank order for the rates of glucuronidation (measured in nmol per min per mg of protein) for genistein was 2.5 μM (0.57 $\pm$ 0.02) > 12.5 μM (0.35 $\pm$ 0.01) > 35 μM (0.27 $\pm$ 0.03) and that for biochanin A was 2.5 μM (0.93 $\pm$ 0.07) > 12.5 μM (0.37 $\pm$ 0.01) > 35 μM (0.27 $\pm$ 0.03)

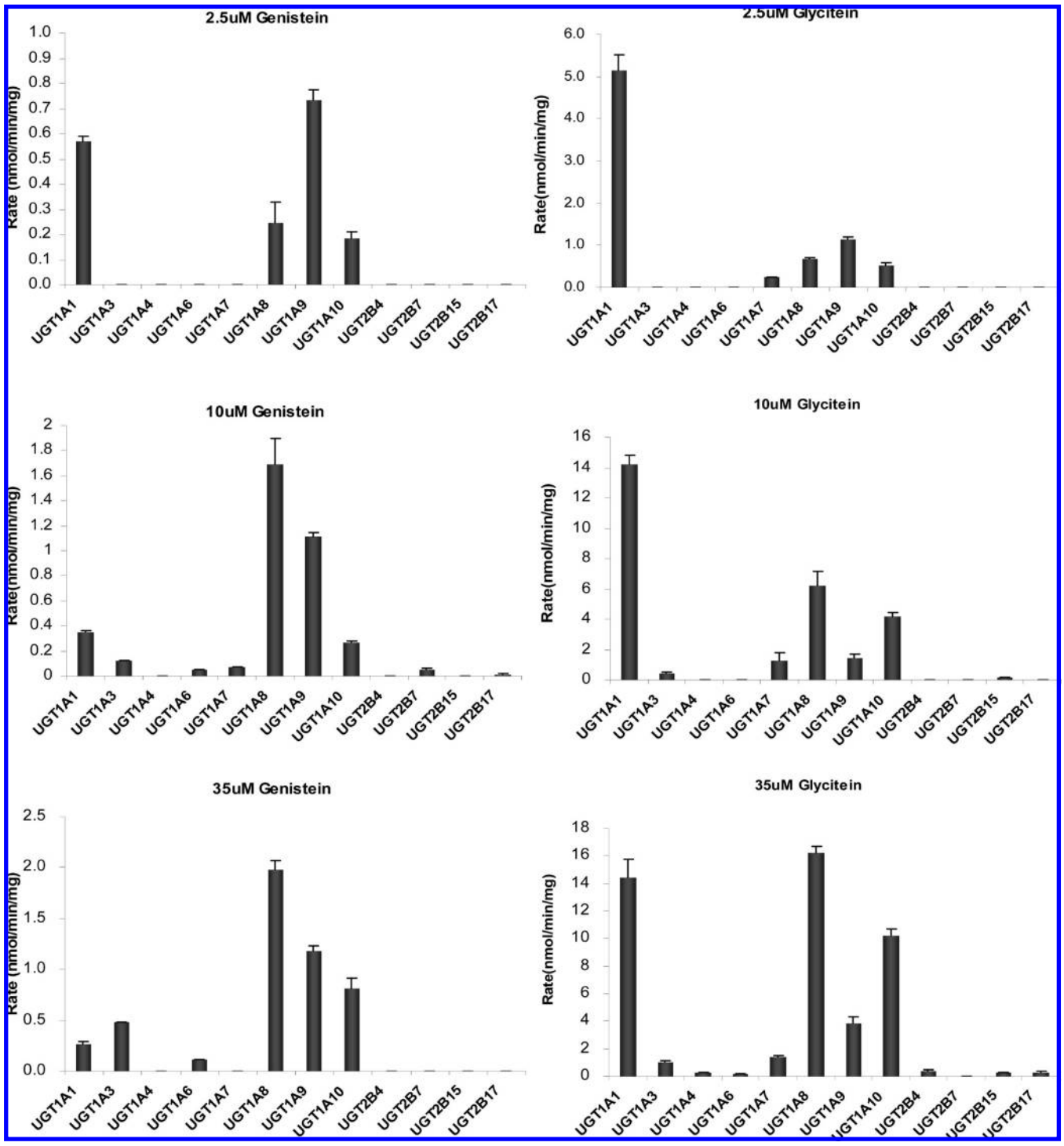

Figure 3. Glucuronidation of genistein and glycitein by expressed human UGTs. Experiments were conducted at three concentrations (2.5 μM, 10 μM and 35 μM). Both genistein and glycitein produced a metabolite 2 at 10 μM and 35 μM by using UGT1A10, but amounts of metabolite 2 formed were less than 5% of the amounts of their respective major metabolite 1, so only metabolite 1 is being shown here. The experiments were conducted at 37 °C for 1 h, and the amounts of glucuronides formed were measured using UPLC. Rates of glucuronidation were calculated as nmol/min/mg of protein. Each bar is the average of three determinations, and the error bars are the standard deviations of the mean ($n = 3$).

(Figure 6). Based on known kinetic profile, this probably represented substrate inhibition kinetics (see later).

The second kind of profile showed an increase in the rates of glucuronidation with an increase in substrate concentrations. For example, genistein was glucuronidated by UGT1A8 at the rates of 0.25 ± 0.08, 1.7 ± 0.20 and 1.98 ± 0.09 (nmol per min per mg of protein) at 2.5, 12.5, and 35 μM genistein concentrations, respectively (Figure

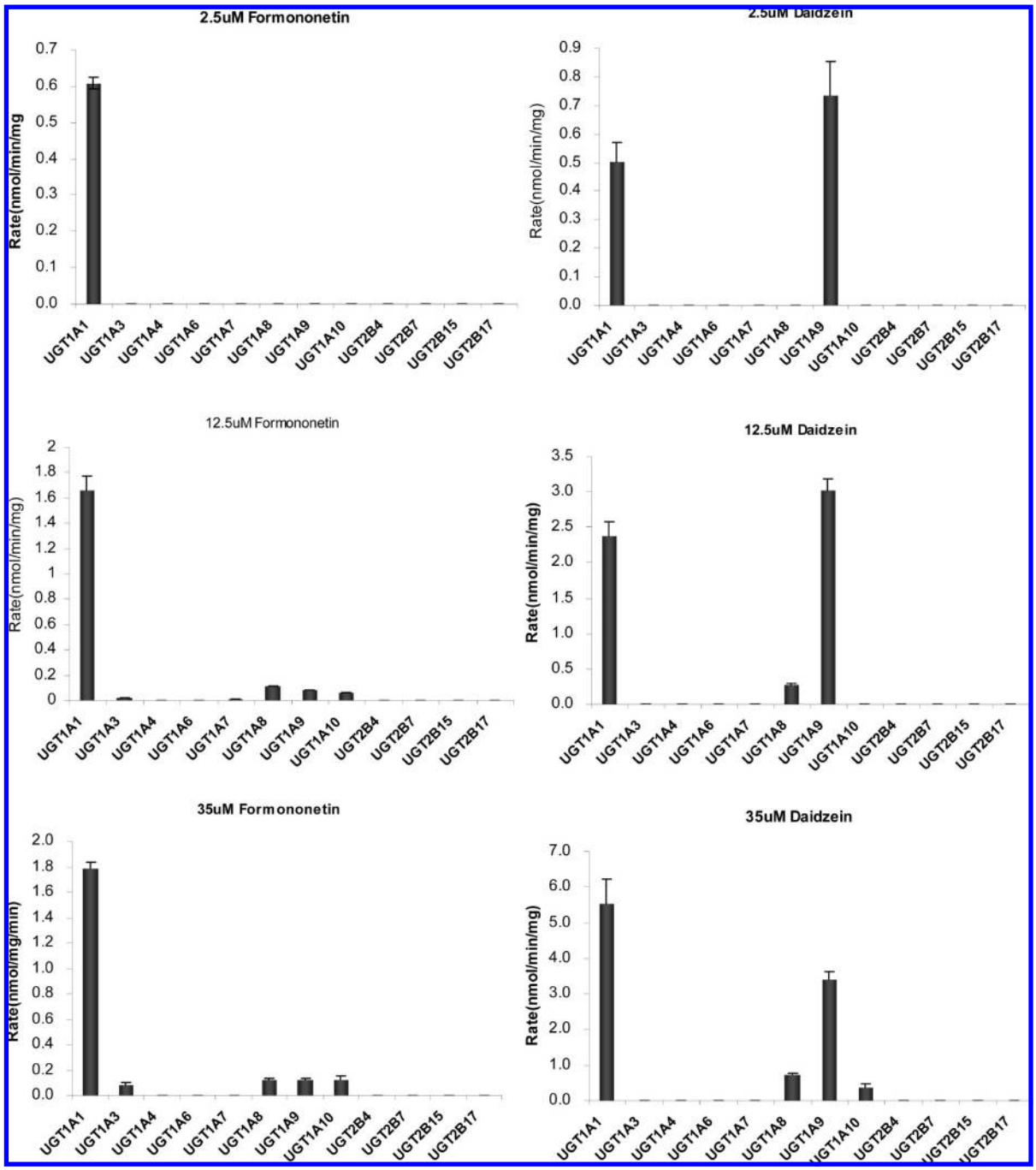

Figure 4. Glucuronidation of formononetin and daidzein by expressed human UGTs. Experiments were conducted at three concentrations (2.5 μM, 12.5 μM and 35 μM). Both formononetin and daidzein produced a metabolite 2 at 12.5 μM and 35 μM by using UGT1A1, 1A9 and 1A10, but amounts of metabolite 2 formed were less than 10% of the amounts of their respective major metabolite 1, so only metabolite 1 is being shown here. The experiments were conducted at 37 °C for 1 h and the amounts of glucuronides formed were measured using UPLC. Rates of glucuronidation were calculated as nmol/min/mg of protein. Each bar is the average of three determinations, and the error bars are the standard deviations of the mean ($n = 3$).

6). Based on known kinetic profile, this probably represented simple Michaelis−Menten kinetics (see later).

The third kind of profile showed that the compound was glucuronidated the fastest at the middle substrate concentration, i.e., 12.5 μM. For example, biochanin A was glucuronidated the fastest at 12.5 μM followed by 2.5 and 35 μM, both by UGT1A9 and by UGT1A10 ($p < 0.05$, one way ANOVA)(Figure 6).

Effects of Structural Changes on Isoflavone Glucuronidation by Four Major UGT Isoforms. Expressed UGT1A1, 1A8, 1A9 and 1A10 were shown to be the four most important isoforms for isoflavones glucuronidation at

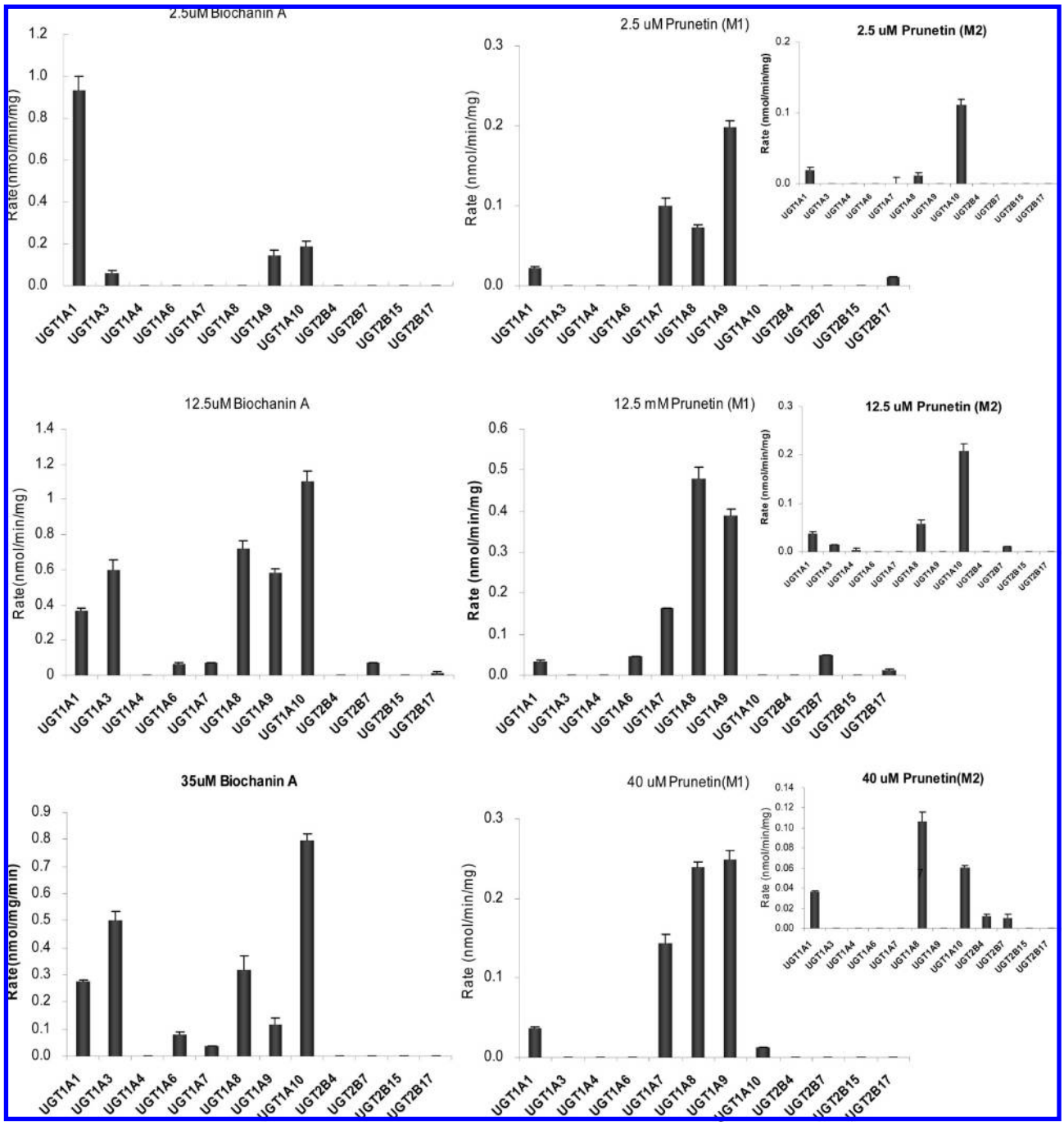

Figure 5. Glucuronidation of biochanin A and prunetin by expressed human UGTs. Experiments were conducted at three concentrations (2.5 μM, 12.5 μM and 35 μM or 40 μM for prunetin). The experiments were conducted at 37 °C for 1 h, and the amounts of glucuronides formed were measured using UPLC. Rates of glucuronidation were calculated as nmol/min/mg of protein. Glucuronidation of prunetin by expressed human UGTs has been adopted from our previous publication for comparison.[12] Insets show relevant formation rates of prunetin-4′-*O*-glucuronide or M2. Each bar is the average of three determinations, and the error bars are the standard deviations of the mean ($n = 3$).

all three selected concentrations. Here we determined how changes in chemical structures affected the glucuronidation rates (Figure 7).

For UGT1A1, at 2.5 μM substrate concentration, glucuronidation of glycitein was the fastest (5.15 $\pm$ 0.35 nmol per min per mg of protein), followed by biochanin A (0.93 $\pm$ 0.07), formononetin (0.61 $\pm$ 0.02), genistein (0.57 $\pm$ 0.02), daidzein (0.50 $\pm$ 0.07), and prunetin (0.02 $\pm$ 0.002). At 12.5 and 40 μM substrate concentrations, the trend was approximately the same, but there was a bigger difference between the slowest and the fastest glucuronidation rates (Figure 7).

For UGT1A8, at 2.5 μM substrate concentration, glycitein was glucuronidated at the fastest rate (0.68 $\pm$ 0.03 nmol per min per mg of protein), followed by genistein (0.25 $\pm$ 0.08) and prunetin (0.08 $\pm$ 0.003), while biochanin A, formononetin, and daidzein showed no detectable metabolism. At 12.5

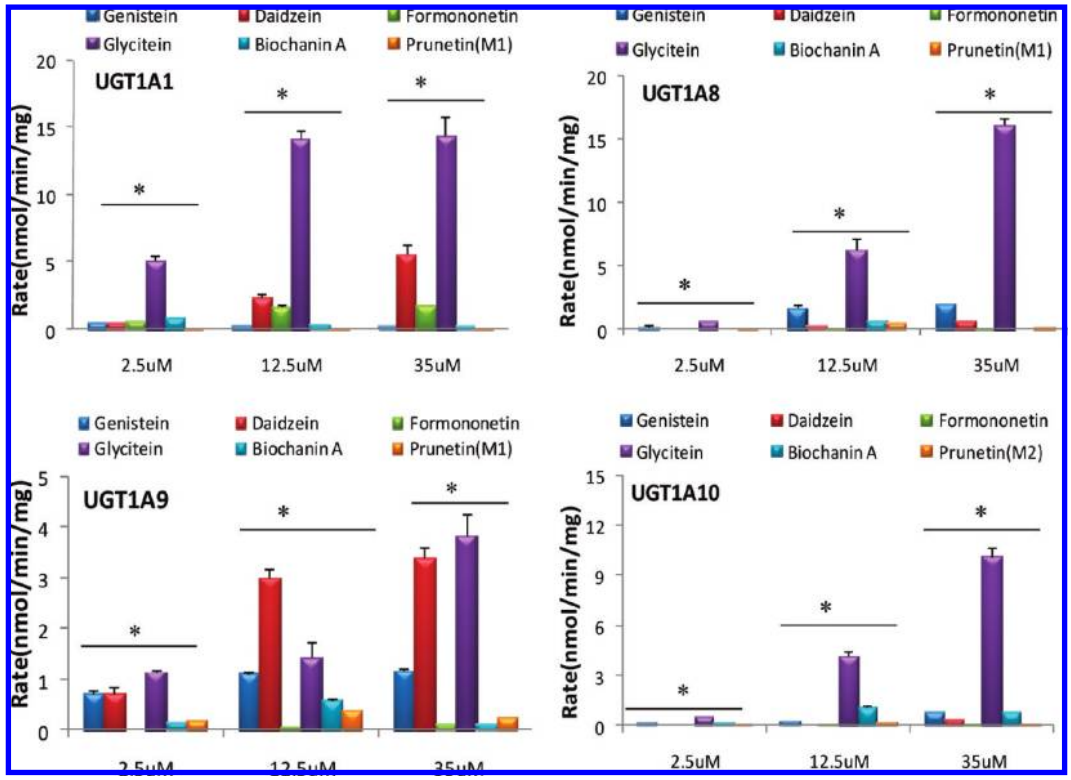

Figure 6. Concentration-dependent glucuronidation of six isoflavones by 4 major human UGTs. Experiments were conducted at three concentrations as designated in Figures 3−5. Each column represents the average of three determinations, and the error bar represents the standard deviation of the mean. Significant differences ($p < 0.05$, one-way ANOVA, marked by *) in rates of glucuronidation were at three different concentrations for each of the isoflavones. Rates of glucuronidation of prunetin by expressed human UGT1A1, UGT1A8, UGT1A9 and UGT1A10 have been adopted from our previous publication for comparison.[12]

and 40 μM substrate concentrations, the isoflavone-specific metabolic profile did not change very much, but differences between the fastest and the slowest glucuronidation rates increased compared to that at the 2.5 μM substrate concentration (Figure 7).

For UGT1A9, at 2.5 μM substrate concentration, the rank order of the UGT1A9-mediated glucuronidation rates (nmol per min per mg of protein) was glycitein (1.15 ± 0.04) > daidzein (0.73 ± 0.12) > genistein (0.73 ± 0.04) > prunetin (0.21 ± 0.01) > biochanin A (0.15 ± 0.02) > formononetin (0.0 ± 0.00). At 12.5 μM substrate concentration, the rank order changed to daidzein (3.03 ± 0.16) > glycitein (1.45 ± 0.28) > genistein (1.16 ± 0.03) > biochanin A (0.59 ± 0.02) > prunetin (0.41 ± 0.01) > formononetin (0.08 ± 0.00). At 35 μM (40 μM for prunetin) substrate concentration, metabolism rates of glycitein (3.85 ± 0.43) became the fastest again but the rank order of metabolism of other isoflavones did not change from those at the 12.5 μM substrate concentration (Figure 7).

For UGT1A10, at 2.5 μM substrate concentration, glycitein was again glucuronidated at the fastest rate (0.52 ± 0.07 nmol per min per mg of protein, $p < 0.05$), followed by genistein and biochanin A, whereas formononetin, prunetin and daidzein showed no detectable metabolism. At 12.5 and 35 μM substrate concentration, glycitein was again glucuronidated at the fastest rate, and the rest of the isoflavone-specific profile showed minimal differences (Figure 7).

Kinetics of Isoflavone Glucuronidation by Four Major UGT Isoforms. We hypothesized that the reason why each isoflavone showed different concentration-dependent metabolic "fingerprint" was because their kinetic parameters (i.e., K_m and V_{max} values) were isoform-dependent. To confirm this hypothesis, the kinetics of genistein and prunetin glucuronidation was determined using concentration versus rates of metabolism and Eadie−Hofstee plots (Figures 8 and 9).

For genistein, UGT1A9- and 1A10-mediated glucuronidation followed classic Michaelis−Menten kinetics, whereas UGT1A8-mediated glucuronidation followed autoactivation kinetics (Figures 8A, 9A−9C). UGT1A1-mediated glucuronidation of genistein was decreased as concentration increased, and its Eadie−Hofstee plot did not match with any known kinetic profile (Figures 8A, 9D). For prunetin, UGT1A7-, 1A9- and 1A10-mediated glucuronidation also followed classic Michaelis−Menten kinetics, whereas UGT1A8-mediated glucuronidation followed autoactivation kinetics (Figures 8B, 9E−9H).

The kinetic parameters were determined for both Michaelis−Menten and autoactivation kinetic profiles using Adapt II

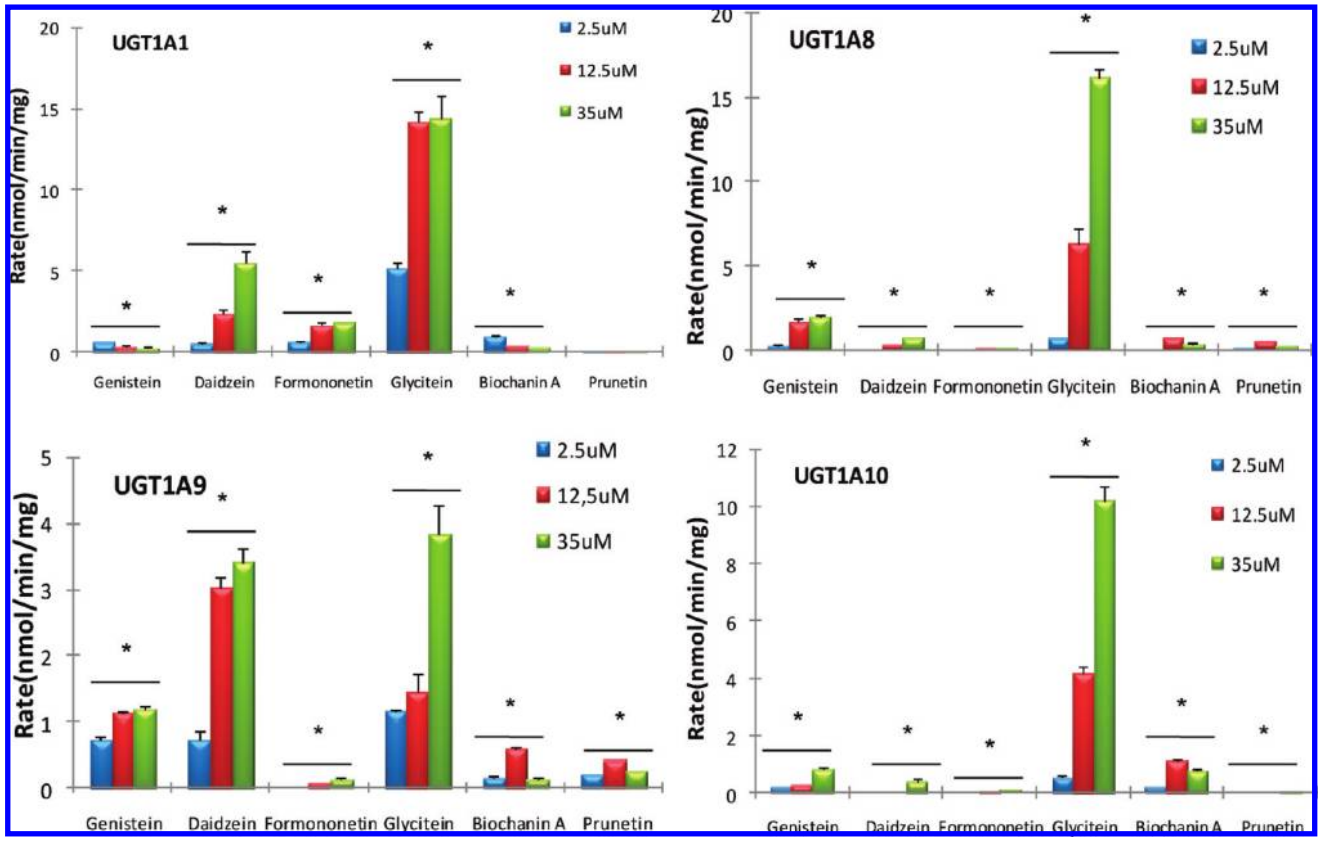

Figure 7. Impact of structural changes on isoflavone glucuronidation by four major UGT isoforms. Experiments were conducted at three concentrations as designated previously in Figures 3−5. Each column represents the average of three determinations, and the error bar represents the standard deviation of the mean. Significant differences at each concentration by each UGT were found among the six isoflavones ($p < 0.05$, one-way ANOVA, marked by *). Rates of glucuronidation of prunetin by expressed human UGT1A1, UGT1A8, UGT1A9 and UGT1A10 have been adopted from our previous publication for comparison.[12]

kinetic modeling software. For genistein, V_{max} and Cl_{int} values ($=V_{max}/K_m$) were the highest for UGT1A8, followed by 1A9, followed by 1A10, while K_m values had the exact opposite rank order (Table 1). For prunetin, Cl_{int} values showed the rank order UGT1A8 > 1A9 > 1A1> 1A10, however V_{max} and K_m values did not follow the same order in any direction (Table 2).

Isoflavone Glucuronidation by Human Liver Microsomes. The rates of glucuronidation of the selected isoflavones by human liver microsomes were determined at three concentrations of 2.5 μM, 12.5 μM and 35 μM (Figure 10A). Previously published research in our lab had shown that prunetin was glucuronidated mainly to metabolite 1 (M1 or prunetin-5-*O*-glucuronic acid) in liver, and to metabolite 2 (M2 or prunetin-4′-*O*-glucuronic acid) in intestine.[12] The results of this study showed that the rate of glucuronidation of glycitein was always the highest of all isoflavones at all of the three substrate concentrations, while prunetin (M1) was glucuronidated the lowest by human liver microsomes.

At 2.5 μM substrate concentration, the rank order of the glucuronidation rates (nmol per min per mg of protein) was glycitein (2.66 ± 0.06) > formononetin (1.71 ± 0.02) > biochanin A (1.20 ± 0.02) > genistein (0.87 ± 0.03) > daidzein (0.75 ± 0.01) > prunetin (0.17 ± 0.01). At 12.5 μM and 35 μM (40 μM for prunetin) substrate concentrations, the rank order of the glucuronidation rates (nmol per min per mg of protein) was essentially maintained although daidzein's rank order was elevated (or more aglycon was metabolized) when compared with those at 2.5 μM substrate concentration.

The results clearly indicated that, at different concentrations, there were significant differences in the glucuronidation of the six isoflavones by human liver microsomes ($p < 0.05$, one way ANOVA) (Figure 10A). In addition, the effects of concentration also showed different trends as we observed in UGT isoforms; namely, glucuronidation rates increased with concentration except in biochanin A, whereas glucuronidation rates decreased with increase in concentration.

Isoflavone Glucuronidation by Human Intestinal Microsomes. When compared to glucuronidation by human liver microsomes, human intestinal microsomes usually metabolized the isoflavones much faster with typical rates at least 2 times faster (Figure 10B). The maximum difference was found in prunetin metabolism, because liver microsomes nearly did not form prunetin-4′-glucuronide but intestinal microsomes made a lot of this metabolite. The apparent rate of prunetin glucuronidation in intestinal microsomes was about 20-fold higher than liver (Figure 10B).

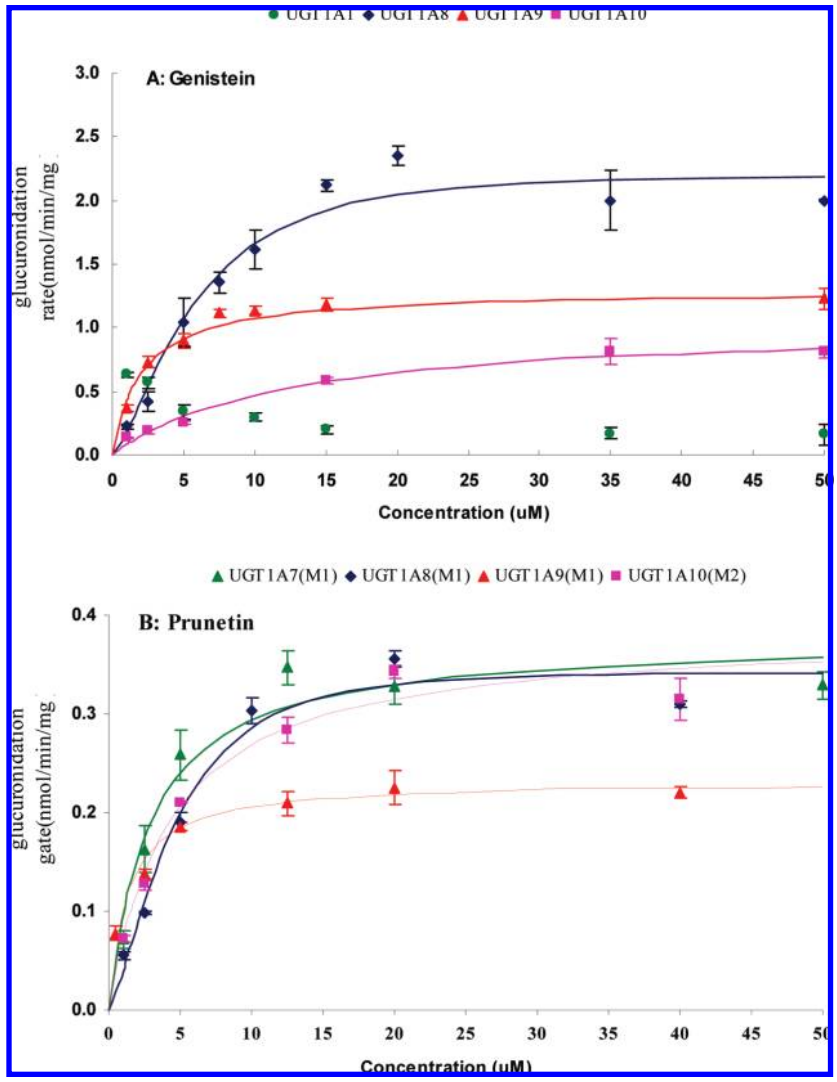

Figure 8. Kinetics of genistein (A) and prunetin (B) glucuronidation by UGT1A1, UGT1A8, UGT1A9 and UGT1A10 (A) ($n = 3$). Rates of glucuronidation were determined at a concentration range of 1 to 50 μM and reaction time of 1 h. The glucuronidation rates are the average of three determinations, and the error bar represents the standard deviation of the mean. The points are the observed isoflavone glucuronides(s) formation rates at different substrate concentrations. The curves are estimated based on fitted parameters generated by the Michaelis−Menten (MM) equation and the other equations describing non-MM enzyme kinetics using software described in the Materials and Methods section. The curve of UGT1A1 does not fit any known model. The apparent kinetic parameters are listed in Tables 1 and 2.

When metabolism rates of six isoflavones in intestine were compared, we found that, at 2.5 μM, formononetin and biochanin A were metabolized the fastest (≈7 nmol per min per mg of protein), followed by glycitein and genistein, prunetin, and daidzein. At 12.5 μM substrate concentration, the rank order changed quite significantly, and glycitein and formononetin showed the highest metabolism rates (≈9 nmol per min per mg of protein). At 35 μM (40 μM for prunetin) substrate concentration, the rank order was essentially the same as observed at 12.5 μM, except that formononetin was metabolized faster than glycitein (Figure 10B).

The results also clearly indicated differences in the effects of substrate concentrations on the glucuronidation of the six isoflavones by human intestinal microsomes ($p < 0.05$, one way ANOVA) (Figure 10B). In addition, the effects of concentration also showed different trends as compared to trends observed with different UGT isoforms; namely, glucuronidation rates of two isoflavones (daidzein and formononetin) increased with concentration, two isoflavones (biochanin A and prunetin) did not change with concentration, and the remaining two (genistein and glycitein) first went up and then came down as the concentration increased (Figure 10B).

Discussion

Our metabolic profiling studies have clearly shown that each isoflavone had a distinctive UGT isoform-specific metabolic pattern that could be used to define or charac-

Table 1. Apparent Kinetic Parameters of Metabolism of Genistein by UGT1A1, UGT1A8, UGT1A9 and UGT1A10, Calculated Based on Curve Fitting Using Michaelis−Menten (MM) and Autoactivation Enzyme Kinetics Models as Described in the *Materials and Methods* Section

kinetic parameters	UGT1A1	UGT1A8	UGT1A9	UGT1A10
K_m (μM)	*a*	1.24	2.09	12.34
V_{max} (nmol/min/mg)	*a*	2.24	1.29	1.04
V_{max}/K_m (mL /min/mg)	*a*	1.81	0.62	0.08
R^2	*a*	0.96	0.98	0.99
AIC	*a*	−7.98	−26.91	−25.23
R (autoactivation only)	*a*	0.18		
$V_{max\text{-}0}$ (autoactivation only) (nmol/min/mg)	*a*	0.01		
$V_{max\text{-}d}$ (autoactivation only) (nmol/min/mg)	*a*	1.23		

[a] Eadie−Hofstee plot of genistein by UGT1A1 does not conform to any known model, so apparent kinetic parameters were not calculated.

Table 2. Apparent Kinetic Parameters of Metabolism of Prunetin by UGT1A7, UGT1A8, UGT1A9 and UGT1A10, Calculated Based on Curve Fitting Using Michaelis−Menten (MM) and Autoactivation Enzyme Kinetics Models as Described in the *Materials and Methods* Section

kinetic parameters	UGT1A7	UGT1A8	UGT1A9	UGT1A10
K_m,(μM)	3.06	0.82	1.29	4.27
V_{max} (nmol/min/mg)	0.39	0.35	0.23	0.38
V_{max}/K_m (mL/min/mg)	0.13	0.42	0.18	0.09
R^2	0.92	0.97	0.97	0.96
AIC	−26.84	−37.19	−41.63	−32.25
R (autoactivation only)		0.22		
$V_{max\text{-}0}$ (autoactivation only) (nmol/min/mg)		0.00		
$V_{max\text{-}d}$ (autoactivation only) (nmol/min/mg)		0.35		

terize a metabolic "fingerprint." Because this "fingerprint" was always dependent on isoflavone structure and frequently on isoflavone concentrations (Figures 3−5), it allowed us to gain a better understanding of isoflavone metabolic processes. It also had a variety of general utilities as described in great detail below. Our studies represent major advances in this area, since previous studies of this type have used fewer compounds,[12,15] fewer UGT isoforms or both.[22] Most studies also used just one or two isoflavone concentrations.[22]

The first utility was to predict the potential of drug−drug interactions and the impact of genetic polymorphisms, both of which influence safety and/or efficacy of drugs.[23] Metabolic profiling of phase I metabolic enzymes especially CYP isoforms had been done for an extended period of time, and proven to be very useful for the purpose of safe and effective use of drugs.[24,25] In fact, phase I metabolic profiling is required by FDA as a part of new drug application dossier.[23] A major task here was to define the main UGT isoforms capable of metabolizing isoflavones based on the "fingerprint." The results showed that four UGT1A isoforms mainly shared the responsibilities of metabolizing the selected isoflavones. In other words, isoflavones were just a class of shared substrates for 4 distinctive UGT isoforms. This was quite unusual if we wanted to compare them to the CYP-catalyzed metabolism, where only one or two isoforms were likely to be responsible for the metabolism of a single substrate.[23] Therefore, isoflavones, which were subjected to the rapid metabolism by four UGT isoforms with significant overlapping specificities, should have been quite resistant to metabolic interactions. Indeed, we have observed in rodents that bioavailability of intact isoflavones were very difficult to change using glucuronidation inhibitors such as probenecid (data not shown). Similarly, low potentials for changes in isoflavone bioavailabilities were expected as a result of genetic polymorphism. Hence, if isoflavones were to be developed into drugs, the potential for isoflavone−drug interaction and impact of genetic polymorphism would be small, a desirable trait for the safe use of drugs.

The second utility of metabolic "fingerprint" was to predict the main organ responsible for the metabolism of isoflavones. This was again done quite frequently for CYP. For example, if a substrate (e.g., debrisoquine[26]) was mainly metabolized by expressed human CYP2D6, which is an isoform mainly expressed in human liver,[26] we could predict that the compound was mainly metabolized in liver. In the present study, the four major isoforms responsible were UGT1A1, 1A8, 1A9 and 1A10. Qualitative and quantitative expression of these UGT isoforms in two main metabolic organ, liver and intestine were quite different.[27] UGT1A1 was expressed in all the organs

(22) Doerge, D. R.; Chang, H. C.; Churchwell, M. I.; Holder, C. L. Analysis of soy isoflavone conjugation in vitro and in human blood using liquid chromatography-mass spectrometry. *Drug Metab. Dispos.* **2000**, *28*, 298–307.

(23) Huang, S. M.; Strong, J. M.; Zhang, L.; Reynolds, K. S.; Nallani, S.; Temple, R.; Abraham, S.; Habet, S. A.; Baweja, R. K.; Burckart, G. J.; Chung, S.; Colangelo, P.; Frucht, D.; Green, M. D.; Hepp, P.; Karnaukhova, E.; Ko, H. S.; Lee, J. I.; Marroum, P. J.; Norden, J. M.; Qiu, W.; Rahman, A.; Sobel, S.; Stifano, T.; Thummel, K.; Wei, X. X.; Yasuda, S.; Zheng, J. H.; Zhao, H.; Lesko, L. J. New era in drug interaction evaluation: US Food and Drug Administration update on CYP enzymes, transporters, and the guidance process. *J. Clin. Pharmacol.* **2008**, *48*, 662–70.

(24) Murray, M. Role of CYP pharmacogenetics and drug-drug interactions in the efficacy and safety of atypical and other antipsychotic agents. *J. Pharm. Pharmacol.* **2006**, *58*, 871–85.

(25) Singh, S. S. Preclinical pharmacokinetics: an approach towards safer and efficacious drugs. *Curr. Drug Metab.* **2006**, *7*, 165–82.

(26) Frank, D.; Jaehde, U.; Fuhr, U. Evaluation of probe drugs and pharmacokinetic metrics for CYP2D6 phenotyping. *Eur. J. Clin. Pharmacol.* **2007**, *63*, 321–33.

(27) Ohno, S.; Nakajin, S. Determination of mRNA expression of human UDP-glucuronosyltransferases and application for localization in various human tissues by real-time reverse transcriptase-polymerase chain reaction. *Drug Metab. Dispos.* **2009**, *37*, 32–40.

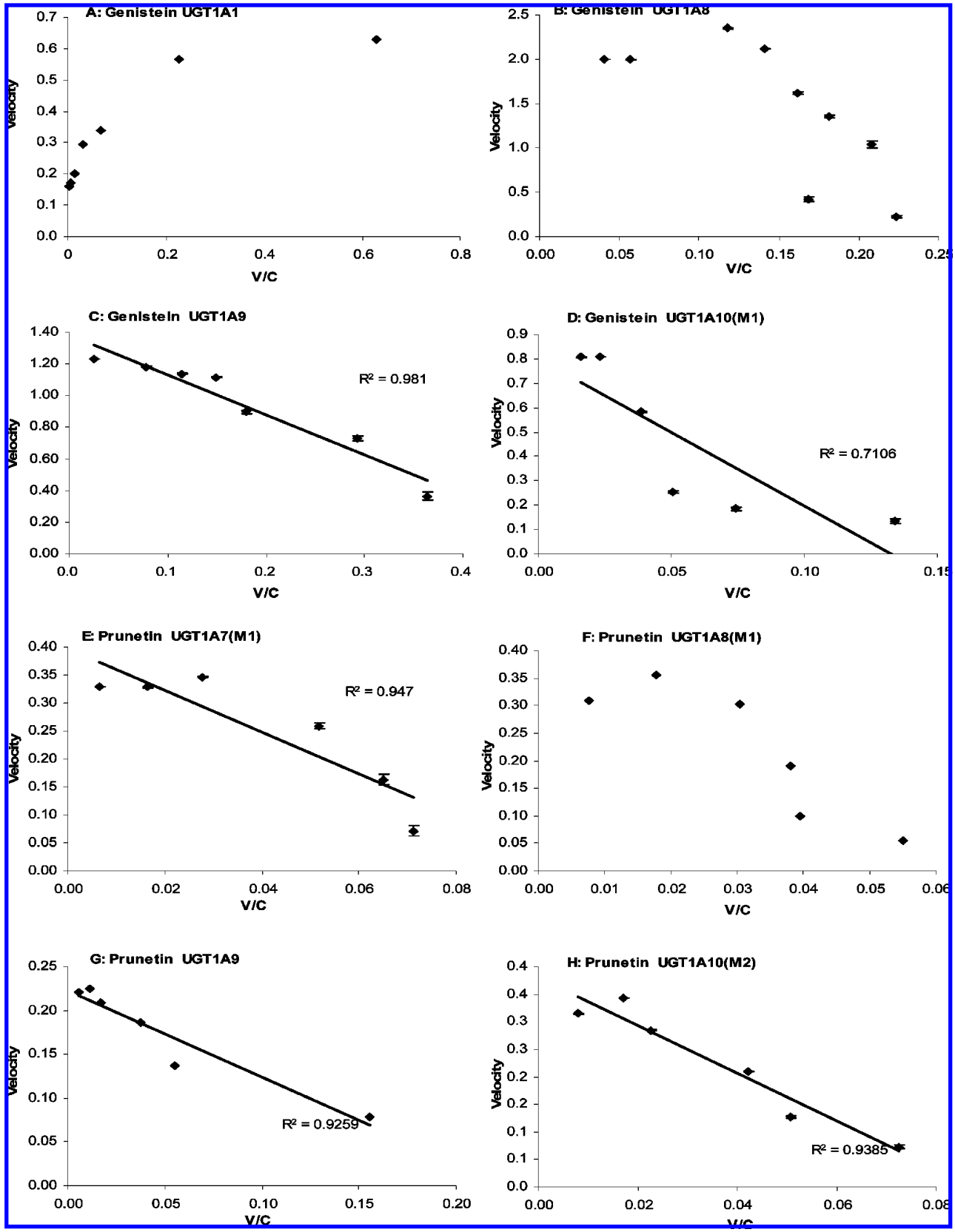

Figure 9. Eadie−Hofstee plots of glucuronidation kinetics shown in Figure 8. For prunetin, UGT1A7, 1A9 and 1A10 showed classic Michaelis−Menten (MM) kinetics, while UGT1A8 showed autoactivation kinetics. Similarly for genistein, UGT1A9 and 1A10 showed classic MM kinetics, while UGT1A8 showed autoactivation kinetics. The Eadie−Hofstee plot of genistein by UGT1A1 does not conform to any known model. The glucuronidation rates are the average of three determinations, and the error bar represents the standard deviation of the mean.

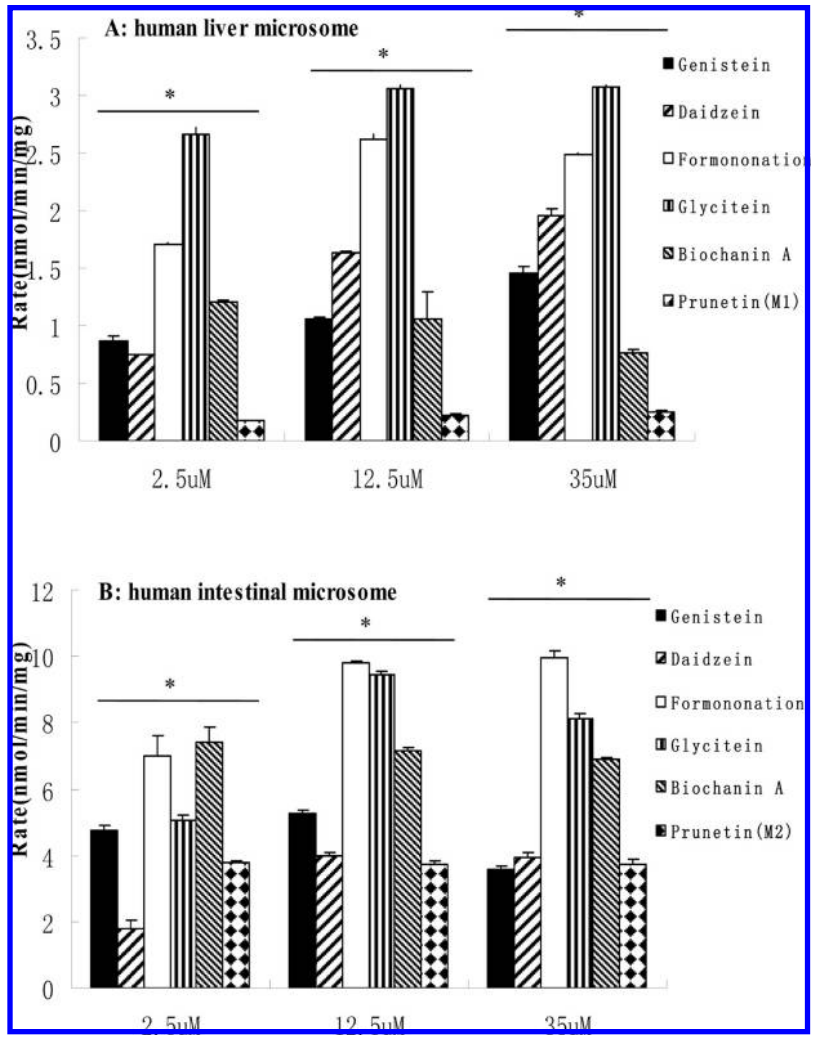

Figure 10. Glucuronidation of six isoflavones by pooled human liver (A) and intestinal (B) microsomes. Three different concentrations (2.5, 12.5, and 35 μM) of substrates were used to determine the rates of metabolism. Each column represents the average of three determinations, and the error bar represents the standard deviation of the mean. Significant differences at each concentration by each UGT were found among the six isoflavones ($p < 0.05$, one-way ANOVA, marked by *).

although its expression in the liver appeared to be more pronounced than that in the intestine.[26] UGT1A9 was only expressed in liver whereas UGT1A8 and UGT1A10 were mostly expressed in the small intestine. Therefore, based on the UGT metabolic fingerprinting of the isoflavones, we predicted, at high isoflavone concentrations (>10 μM), the main organ of metabolism for genistein, glycitein, biochanin A and prunetin to be the intestine (microsomes) and the main organ of metabolism for formononetin and daidzein (more so for daidzein) to be the liver (microsomes). The prediction for the first four isoflavones turned out to be right, but for the second two isoflavones, it appeared to be incorrect. Prediction for formononetin also fell short in the extent of metabolism aspect (discussed later). We believed this was due to the absence of a metabolic "fingerprint" or a certain major UGT isoform(s), which was especially capable of rapidly metabolizing isoflavones lacking a 5-OH or 6-OCH_3 group (i.e., daidzein, glycitein and formononetin). We speculated that the recently characterized UGT3A1 might be involved since this isoform metabolizes phenols such as nitrophenol and estradiol (estrogens).[28] Additional studies are necessary to identify which UGT isoforms are capable of rapidly metabolizing flavonoids without 5-OH or 6-OCH_3 group.

The third utility of the metabolic "fingerprint" was to predict the extent of metabolism and metabolic rank-order in target tissues (e.g., intestine and liver). Based on Figure 11A, this would have translated into rapid metabolism of glycitein, daidzein, and genistein, as well as slow metabolism of biochanin A, formononetin and prunetin in tissues. In liver microsomes, the prediction was essentially accurate for glycitein, genistein and prunetin and reasonable for biochanin A and daidzein. A correlation between

(28) Mackenzie, P. I.; Rogers, A.; Treloar, J.; Jorgensen, B. R.; Miners, J. O.; Meech, R. Identification of UDP glycosyltransferase 3A1 as a UDP N-acetylglucosaminyltransferase. *J. Biol. Chem.* **2008**, *283* (52), 36205–10.

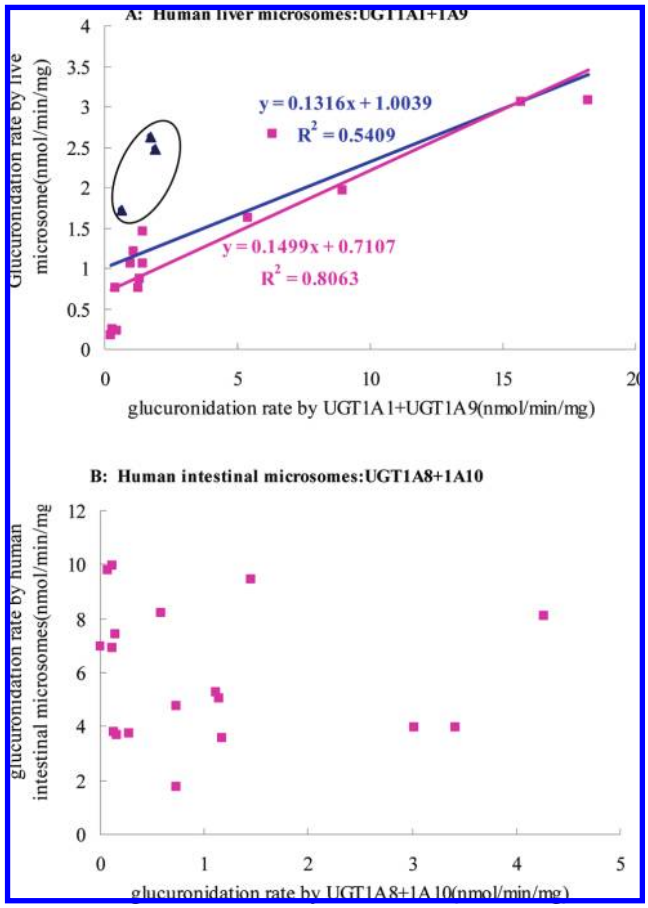

Figure 11. Correlation of glucuronidation rates obtained from 2 UGTs with those obtained from human liver (A) and intestinal (B) microsomes. Linear regression was used to derive apparent correlations. In panel A, the blue line (R^2 = 0.54) is the one with all six isoflavones, whereas the pink line (R^2 = 0.81) is the one without formononetin (data for UGT glucuronidation for formononetin at three concentrations are shown in the circle).

the rates of glucuronidation of six isoflavones by human liver microsomes and the combined rates of glucuronidation by UGT1A1 and UGT1A9 together was established (Figure 11A). UGT1A1 and UGT1A9 were chosen together for establishing correlation, as they were among the most abundantly expressed isoforms in human liver, which contribute significantly to isoflavone metabolism. The results showed a moderate correlation coefficient of 0.54 when data of all six isoflavones was plotted, whereas the correlation coefficient was significantly improved to 0.8, when data was plotted after excluding formononetin rates of glucuronidation (Figure 11A). The fact that we missed on predicting metabolism of formononetin suggested that one (or more) major isoflavone metabolizing UGT isoform(s) was missing from the present "fingerprint" studies, as stated previously. When the same approach was used to correlate intestinal microsomal metabolism of isoflavones with expressed UGT data, the outcome was unexpected and showed no apparent correlation (Figure 11B). It was uncertain as to why there was no apparent correlation, but we speculated that one of the reasons was that one or more major intestinal UGT isoforms capable of metabolizing isoflavones was missing.

Another use of the metabolic "fingerprint" was to determine structure−activity (metabolism) relationship (SAR/SMR). Since all isoflavones shared the same structural backbone, the SAR/SMR studies mainly examined how changes in the position of methoxy group and hydroxyl group (the site of glucuronidation) affected its glucuronidation by the most important expressed human UGT isoforms: UGT1A1, 1A8, 1A9 and 1A10. Our analysis indicated that prunetin was really different from others because it was the only compound among the six that did not have a 7-OH group. This structural characteristic might have drastically decreased its glucuronidation by UGT1A1 (Figure 6A), but more compounds possessing this structural characteristic may be needed to make an affirmative statement. This lack of metabolism of prunetin was not surprising since it was also shown to be poor substrate for glucuronidation in Caco-2 cells,[11] which expressed multiple UGT1As with UGT1A1 as one of its major UGT isoforms.[15] The "fingerprint" studies of additional UGT isoforms also indicated that UGT2B7 only glucuronidated isoflavones with a 5-hydroxyl group. Therefore, three isoflavones that had a 5-hydroxyl group (genistein, biochanin A and prunetin) were its substrates, and isoflavones without the 5-hydroxyl group (daidzein and formononetin) were not.

Having stated the need for and utilities of "fingerprinting," a relevant question was then what constitutes a reasonable "fingerprint." When studying effects of substrate concentration on metabolic profiling, we found that changes in substrate concentrations could change "fingerprint" and therefore it became necessary to conduct metabolic profiling at multiple concentrations. We have chosen three different concentrations and found that this appeared to be satisfactory. These three concentrations should cover good range with concentration higher and lower than the expected K_m value. The third concentration should be in between. In this case, we used a low concentration of 2.5 μM since a concentration lower than 2.5 μM will hinder quantitation of metabolites via UV. We did not propose to use a high concentration greater than 35 μM because of solubility limits. The medium concentration we used here is 12.5 μM, since this was close to the average of the low and the high. Based on the success we had, we believed that "fingerprint" studies at three concentrations were essential if we wanted to develop a useful "fingerprinting" profile. Another necessary piece of "fingerprinting" was more obvious, which was to have all the fingers. The fact that we missed badly on formononetin metabolism prediction suggested that we did not have all the "fingers" necessary for its fingerprint-

ing. We will conduct additional studies to define what we have missed.

In conclusion, we have shown for the first time that the glucuronidation of six common isoflavones were all UGT isoform-, substrate structure- and concentration-dependent, which can be effectively captured by metabolic "fingerprint" using expressed human UGT isoforms. We demonstrated for the first time the multifaceted utilities of UGT metabolic "fingerprint" in defining drug interaction potentials, genetic polymorphism consequence, major organs for metabolism, and SMR. We believe that the approach developed here may be of general utility in defining the metabolic "fingerprint" of other UGT substrates, which in turn could improve the safety as well as efficacy of drugs that are inactivated (occasionally activated) or eliminated by the glucuronidation pathway.

Abbreviations Used

UGT, UDP-glucuronosyltransferases; UDPGA, uridine diphosphoglucuronic acid; UPLC, ultraperformance liquid chromatography; AIC, Akaike's information criterion; SMR, structure metabolism relationship.

Acknowledgment. This work is supported by NIH GM-070737 to M.H. L.T. is supported in part by a SMU training grant. Z.L. is supported by a 115 Key Project of the Ministry of Science and Technology of PR China (No. 2006BAI11B08-4).

MP8002557